Science Advances

AAAS

advances.sciencemag.org/cgi/content/full/3/9/e1700764/DC1

Supplementary Materials for

A versatile 3D tissue matrix scaffold system for tumor modeling and drug screening

Girdhari Rijal and Weimin Li

Published 13 September 2017, *Sci. Adv.* **3**, e1700764 (2017)
DOI: 10.1126/sciadv.1700764

The PDF file includes:

Other Supplementary Material for this manuscript includes the following:
(available at advances.sciencemag.org/cgi/content/full/3/9/e1700764/DC1)

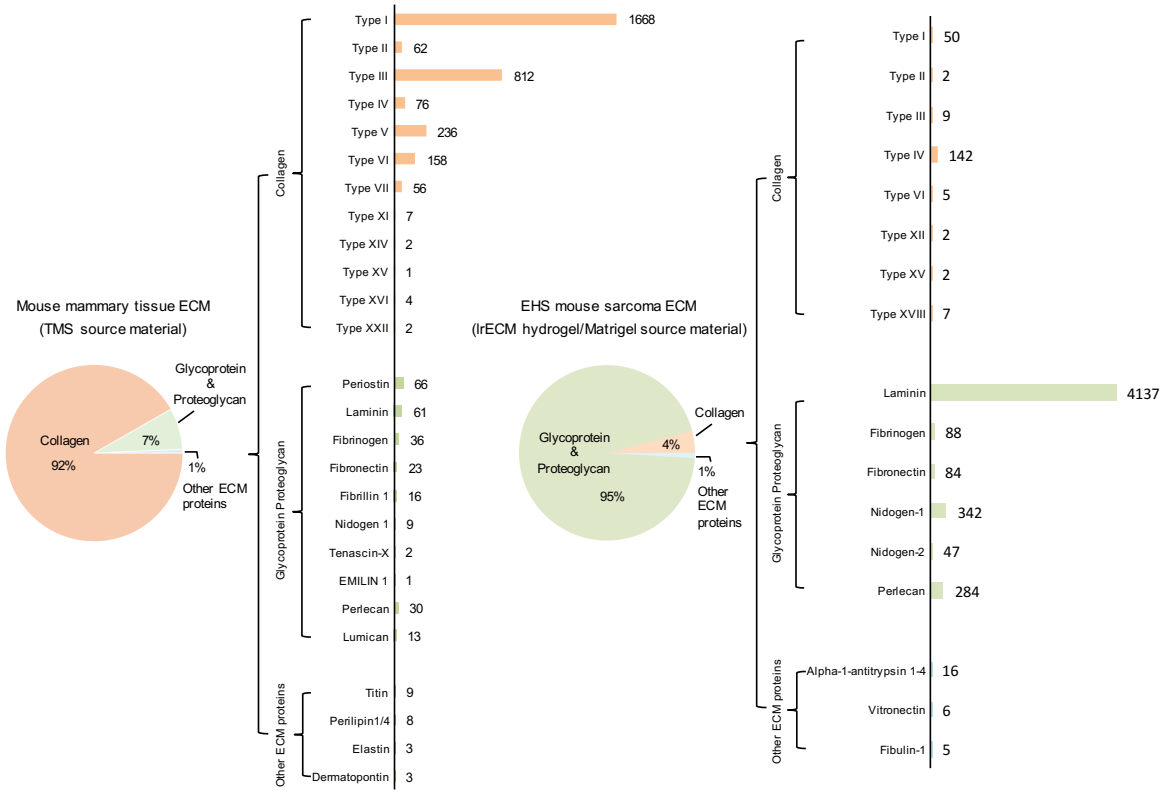

fig. S1. Comparision of the differences of the major proteins identified from TMS/mouse mammary tissue ECM vs. those from IrECM hydrogel. The ECM proteins listed in Table 1 and Supplementary table 1 were grouped and compared side-by-side. The spectrum counts of the different subunits or chains of a same protein were added up to represent the relative abundance of the functional protein within the ECM.

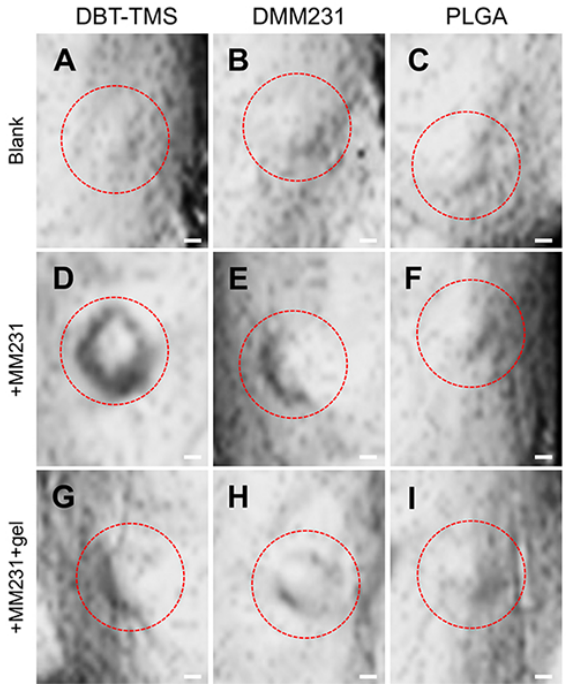

fig. S2. Monitor tumor growth with x-ray-based imaging. CT images of the tumors originated from the 3D scaffolds coated with or without the MM231 cancer cells in the presence or absence of an outer TMS hydrogel layer were taken 3 weeks after implantation of the scaffolds into the animals. Scale bars, 4 mm.

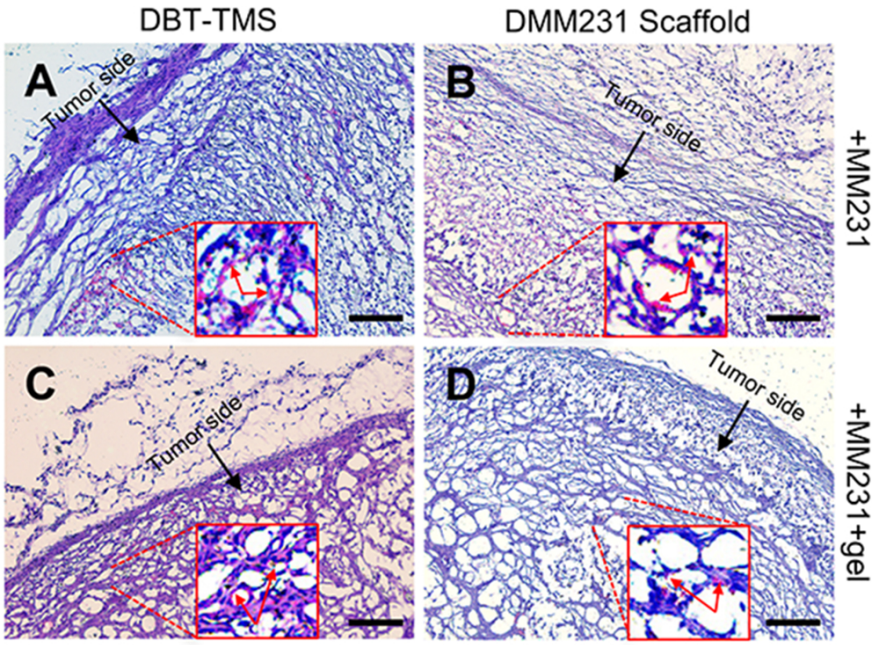

fig. S3. Tumor development from the cancer cell-laden scaffolds in mice mammary tissues. H&E staining of the cross sections of the tumors derived from the

MM231 cell-laden DBT-TMS and DMM231 scaffolds in the presence or absence of a layer of hydrogel covered outside of the seeded cells. The ECM architectures, overall cell distribution and microvessels (blowup insets, with arrows pointed to the red blood cell-containing capillaries) within the tumors are displayed. Scale bars, 100 μm. The representative blowup views of the stained sections were demonstrated in Fig. 4C, i - iv.

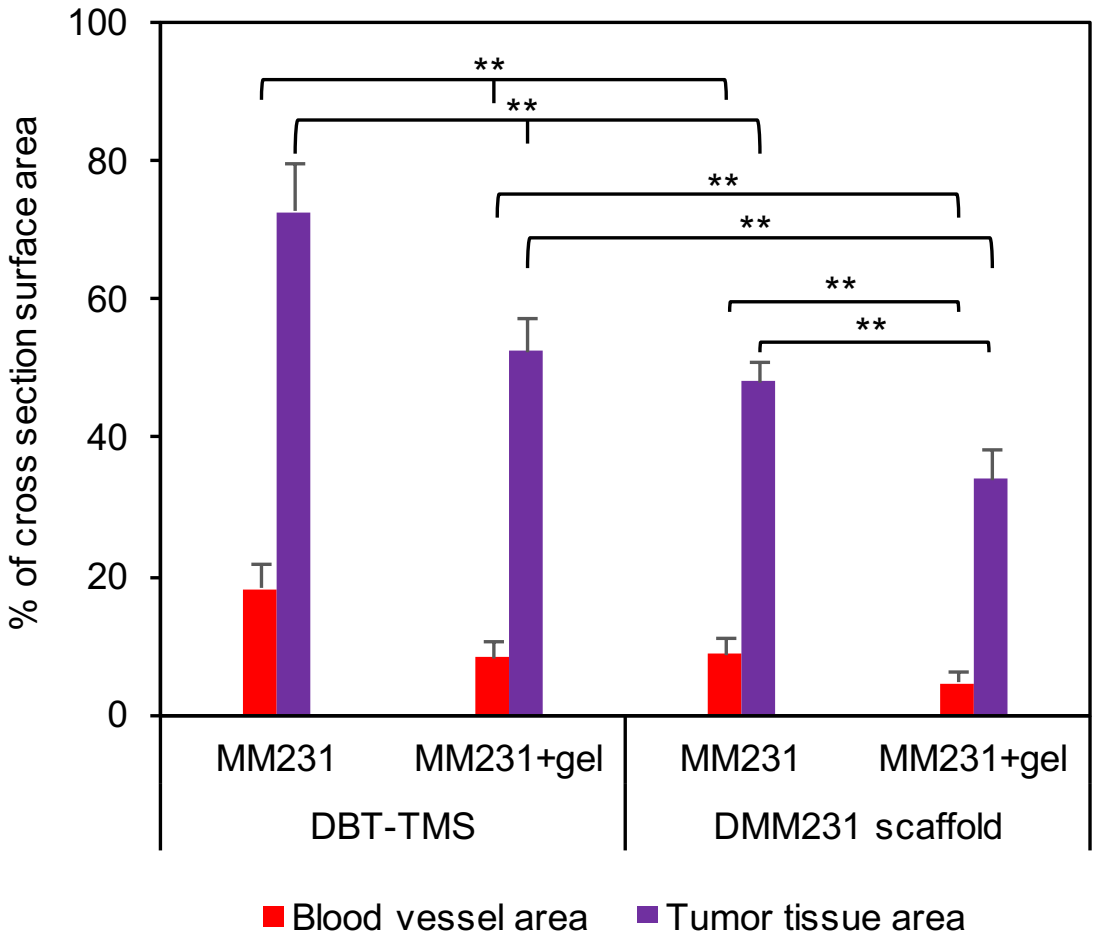

fig. S4. Quantification of the capillary areas on the cross sections of the tumors. H&E stained cross sections of the tumors were analyzed for the occupancies of the blood vessels relative to the solid tumor tissues as described in the methods. Error bars represent the SD of the means of the values from 3 consecutive slides (per tumor) of 3 replicate tumors. **P<0.01: comparisons of the counterpart samples between the

different scaffold groups or the samples within the same scaffold group in the presence or absence of the hydrogel coverage.

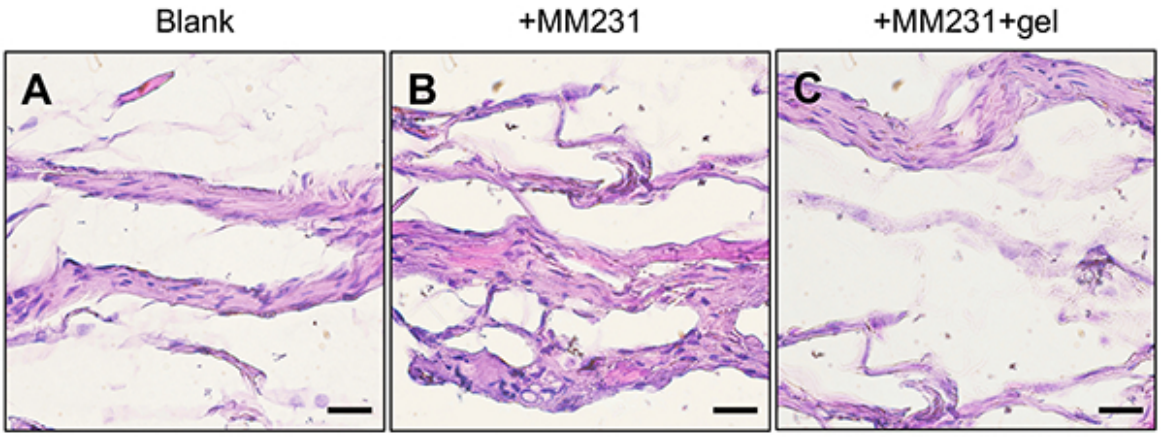

fig. S5. **Histological examination of the tumors developed from the cancer cells grown on the PLGA scaffolds.** H&E staining of the cross sections of the implanted PLGA scaffolds with or without the MM231 cells and a hydrogel outer layer showed underdeveloped and disorganized ECM structures as well as limited cell infiltration into the ECM. Scale bars, 100 μm.

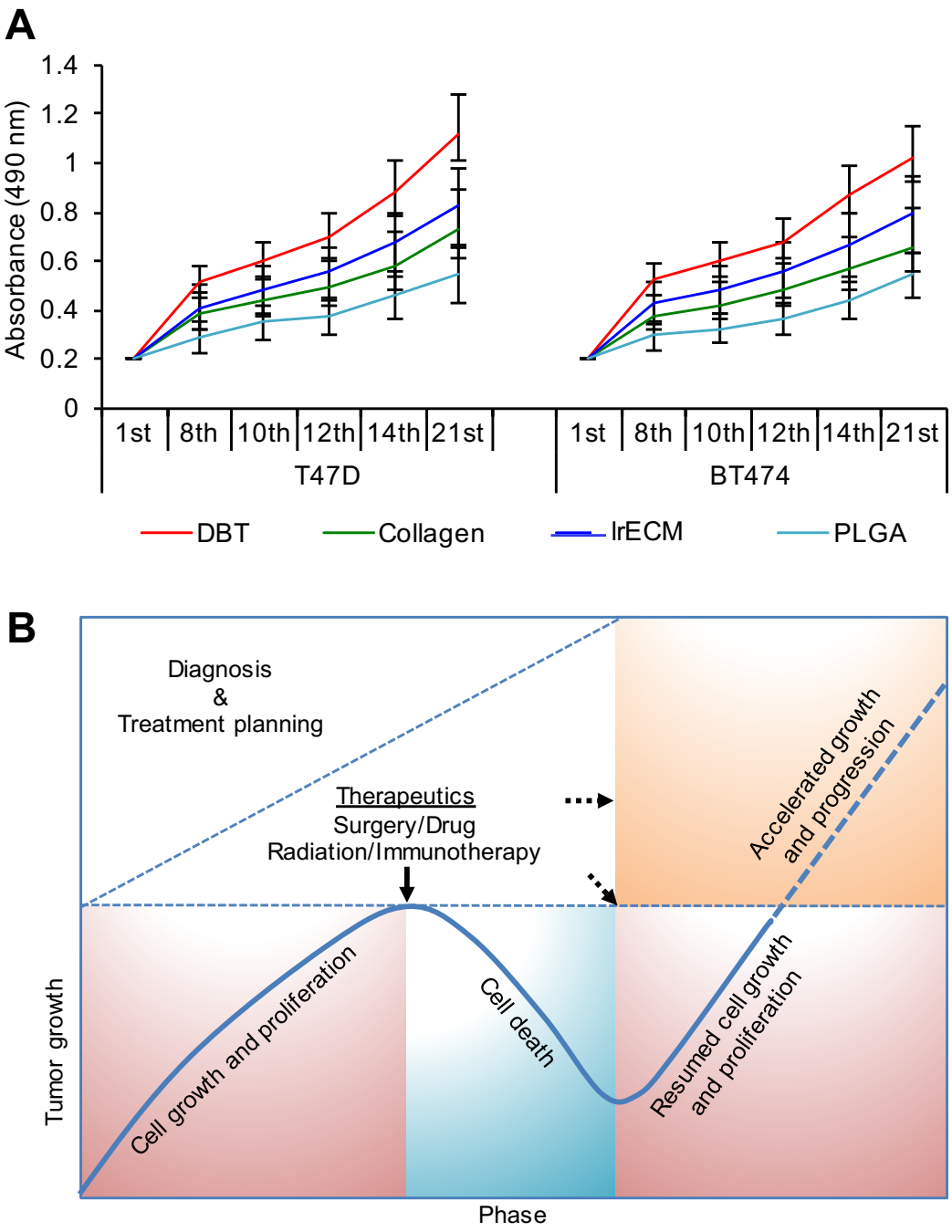

fig. S6. Analysis of T47D and BT474 cell proliferation on the different scaffold as well as the potential of using the systems in drug screening. (A) The proliferation of T47D and BT474 cells grown on the different scaffolds was evaluated with cell proliferation assays. The analysis of the data collected from the indicated time points served as a reference for the drug tests shown in Fig. 5. Error bars represent the SD of the means of 3 independent experiments. **(B)** The clinical trends of tumor development and response to treatment. The tumor growth over the phase of cell

proliferation status in response to therapeutic interventions was depicted. The dotted arrows indicate the additional treatment options during the disease progression.

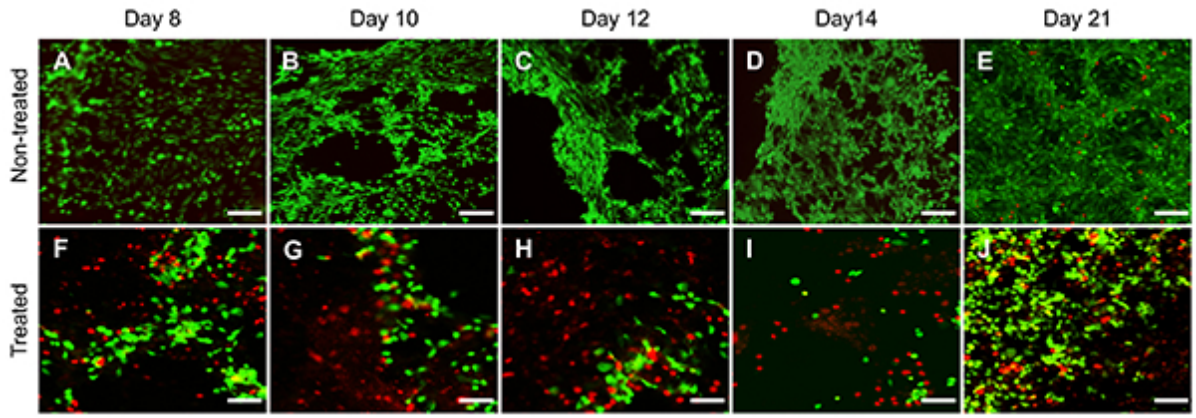

fig. S7. Cancer cell survival and growth status on TMS after drug treatment. In addition to the proliferation assays shown in Fig. 5A, the sensitivities of T47D or BT474 cells grown on the DBT-TMSs to HT or Taxol treatment were inspected using Live/Dead Cell staining at different time points. Only the T47D/TMS ± HT results were shown here, with the similar patterns were observed in the BT474/TMS ± HT and the T47D/TMS ± Taxol or the BT474/TMS ± Taxol samples (data not shown). The green and the red signals indicate the live and the dead cells, respectively. Scale bars,100 μm.

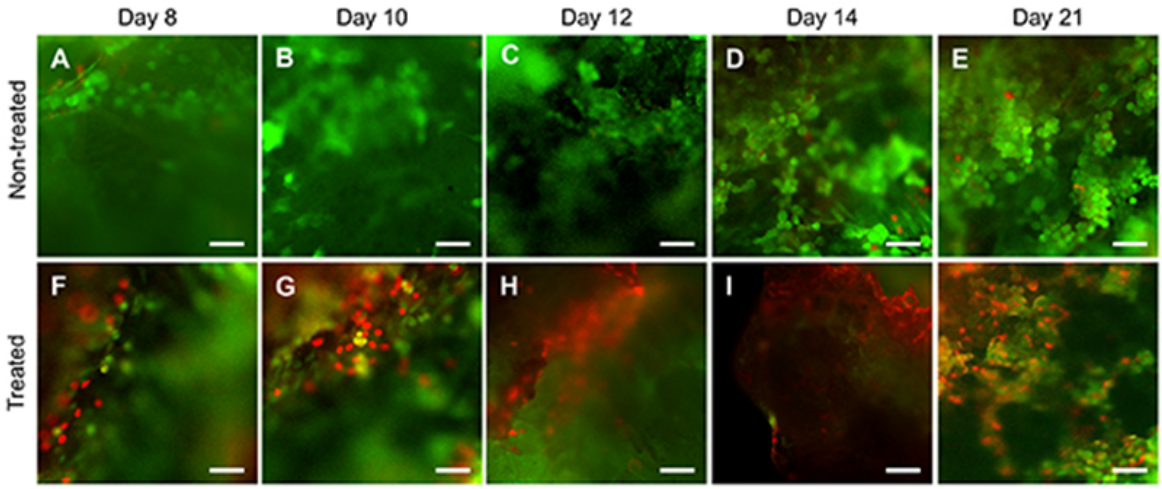

fig. S8. Cancer cell survival and growth status on PLGA scaffolds after drug treatment. The sensitivities of the T47D or BT474 cells grown on the PLGA scaffolds

to the anticancer drugs were assessed with Live/Dead Cell staining at different time points. The results of the T47D/PLGA ± HT samples were displayed, with the similar patterns were observed in the BT474/PLGA ± HT and the T47D/PLGA ± Taxol or the BT474/PLGA ± Taxol samples (data not shown). Scale bars, 150 μm.

table S1. The major proteins identified in the IrECM. The proteins were grouped according to their similarities in a family or functions in the ECM, and listed from high to low spectrum counts.

	#	Protein	Gene	Accession number	Molecular mass (kDa)	Spectrum count
Collagen	1	Collagen type IV alpha 2 chain	Col4a2	P08122	167	87
	2	Collagen type IV alpha 1 chain	Col4a1	P02463	161	55
	3	Collagen type I alpha 1 chain	Col1a1	P11087	138	35
	4	Collagen type I alpha 2 chain	Col1a2	Q01149	130	15
	5	Collagen type III alpha 1 chain	Col3a1	P08121	139	9
	6	Collagen type XVIII alpha 1 chain	Col18a1	E9QPX1	182	7
	7	Collagen type VI alpha 1 chain	Col6a1	Q04857	108	5
	8	Collagen type II alpha 1 chain	Col2a1	P28481	142	2
	9	Collagen type XII alpha 2 chain	Col12a1	Q60847	340	2
	10	Collagen type XV alpha 1 chain	Col15a1	A2AJY2 (+1)	138	2
Glycoprotein & proteoglycan/GAG	11	Laminin subunit alpha 1	Lama1	F8VQ40	338	1567
	12	Laminin subunit gamma 1	Lamc1	F8VQJ3	177	1324
	13	Laminin subunit beta 1	Lamb1	E9QN70 (+1)	202	1205
	14	Laminin subunit alpha 5	Lama5	Q61001	404	28
	15	Laminin subunit beta 2	Lamb2	Q61292	197	10
	16	Laminin subunit alpha 4	Lama4	P97927	202	3
	17	Nidogen-1	Nid1	P10493	137	342
	18	Nidogen-2	Nid2	O88322	154	47
	19	Perlecan	Hspg2	E9PZ16	470	284
	20	Fibronectin	Fn1	P11276	273	84
	21	Fibrinogen beta chain	Fgb	Q8K0E8	55	40
	22	Fibrinogen gamma chain	Fgg	Q8VCM7	49	33
	23	Fibrinogen alpha chain	Fga	E9PV24 (+1)	87	15
Other ECM proteins	24	Alpha-1-antitrypsin 1-4	Serpina1d	Q00897	46	16
	25	Vitronectin	Vtn	P29788	55	6
	26	Fibulin-1	Fbln1	Q08879	78	5

movie S1. Testing the sponginess of the TMS scaffolds. The video showed the sponginess or resilience of the TMS scaffolds, which were able to return to their original shapes after releasing the applied pressure.